

Modelling the fuel reactor of a fluidised bed chemical-looping coal combustor

A.D. Engelbrecht¹, B.C. North¹, B.O. Oboirien¹

¹CSIR Materials Science and Manufacturing, Pretoria, South Africa

Keywords: Chemical-looping combustion, fluidised bed, high-ash coal, modelling

Abstract – Chemical-looping combustion (CLC) of coal has emerged as a clean coal technology that can potentially be applied for the efficient combustion of coal while producing flue gas that has a CO₂ concentration of greater than 99 %. An important component of a CLC combustor is the fuel reactor (FR) where conversion of the coal takes place. A bubbling fluidised bed reactor model originally developed at the CSIR to simulate the gasification of high-ash coal was modified so that it can be used to simulate the FR of a chemical-looping combustor. Simulations were carried out to investigate the effect of coal, oxygen carrier and operating variables on the performance of the FR. Simulations predict that the temperature, pressure, oxygen carrier reactivity, coal reactivity and coal residence time has the greatest effect on the coal conversion efficiency in the fuel reactor.

INTRODUCTION

Since 1880 the average global temperature has increased by ± 0.85 °C. Climate scientists are 95 % sure that more than 50 % of the global warming is as a result of the greenhouse gasses produced by human activity. Carbon dioxide from the combustion of fossil fuels has contributed to 65 % of the enhanced greenhouse gas effect. Without mitigation of CO₂ emissions in future, the global temperature is expected to increase by 4.0 °C above pre-industrial levels by 2100. The risk associated with a 4.0 °C temperature increase by 2100 include substantial species extinction, global and regional food insecurity, increased frequency of extreme weather events and constraints on common human activities. Combustion engineers are therefore making a concerted effort to reduce the amount of CO₂ that is released during energy production from fossil fuels. Avenues that are being explored are to increase power generation efficiencies and to capture CO₂ and store it in the crust of the earth and under the floor of the ocean. Technologies that are being developed to capture CO₂ from power station are: 1) pre-combustion capture, 2) oxy-fuel combustion, 3) post combustion capture and 4) chemical-looping combustion. Techno-economic studies [1, 2] show that options 1 to 3 have efficiency penalties of about 10 % resulting in an increase in the price of energy. The IPCC & IEA identified Chemical-Looping Combustion (CLC) as a CO₂ capture technology that has the potential to reduce the cost of CO₂ capture by 50 % compared to options 1 to 3. The disadvantage of CLC compared to options 1 to 3 is that it is currently in the early stages of development and the confidence in the use the technology is low. The largest CLC demonstration plant is located at the Technical University of Darmstadt and has a thermal output of 1 MW [3].

CHEMICAL-LOOPING COMBUSTION

Chemical-looping combustion uses a metal oxide oxygen carrier (OC) to transfer oxygen from air to a separate reactor (fuel reactor) where it reacts with fuel as shown in Figure 1. By avoiding direct contact of fuel with air, a high concentration (> 99%) of CO₂ in the dry flue gas is obtained since the flue gas is not diluted with nitrogen. Pure CO₂ for sequestration can easily be produced from this stream. In the fuel reactor (FR) the fuel reacts with the OC to produce CO₂ and H₂O and a reduced OC. The reduced OC is transferred to the air reactor (AR) where it is oxidized with air producing heat in the process. The exothermic oxidation of the OC produces a high-temperature stream containing nitrogen and oxygen that is free of CO₂. This stream is used to generate electricity using a boiler and a steam turbine. The temperature of the OC is raised in the AR and can therefore be used to transfer heat to the FR. Circulation of the OC between the AR and the fuel reactor, therefore, transfers oxygen and heat from the air reactor to the fuel reactor. Fluidised beds are the technology of choice for the AR and the FR in CLC due to the ease with which the OC can be circulated between the AR and the FR. A fast fluidised bed is most suitable for the AR since it facilitates the transfer of OC from the AR to the FR via a cyclone and standpipe. To allow the redox reactions to proceed to completion longer OC residence times are required in the FR compared to the AR. For this reason bubbling and circulating fluidised beds are often used for the FR.

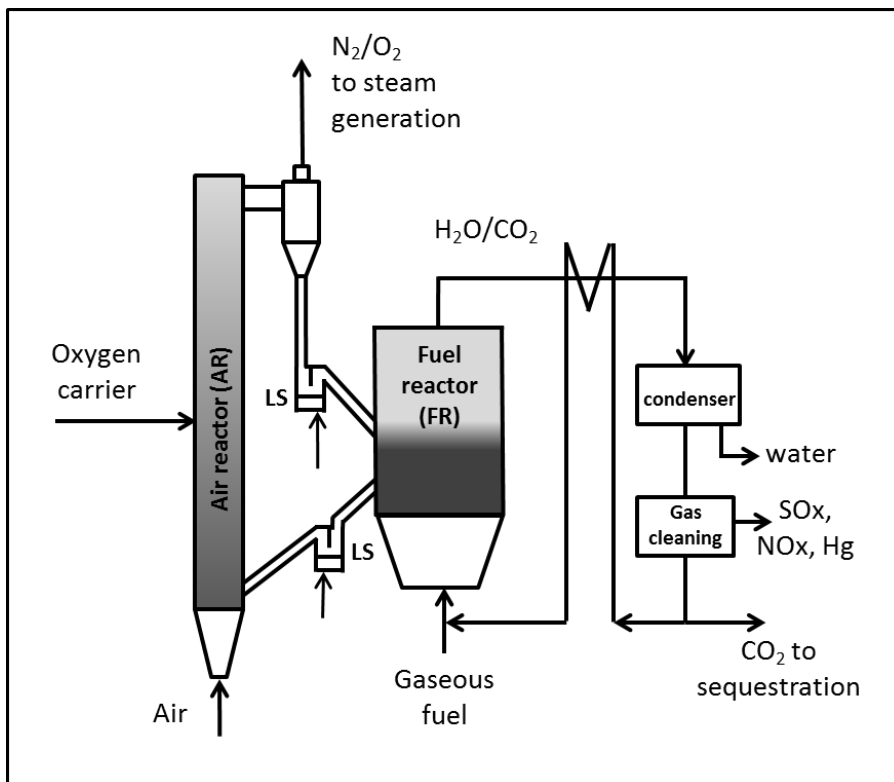


Figure 1. Chemical-looping combustion of gaseous fuels

During the initial stages of CLC development, the combustion of gaseous fuels such as natural gas (CH₄) and syngas (CO, H₂, CH₄) was investigated (Figure 1). Due to the large reserves of solid fuels such as coal, CLC research has been extended to these fuels. Figure 2 shows a flow diagram of a CLC system for the combustion of coal. In this process the FR is fluidised by gasification agents (CO₂ and H₂O). Gasification of coal takes place in the FR, and the resulting gasses (CO, H₂, and CH₄) are oxidized by the OC producing CO₂ and H₂O. Due to the relatively slow rate of the gasification reactions unconverted char leaves the FR with the circulating oxygen carrier.

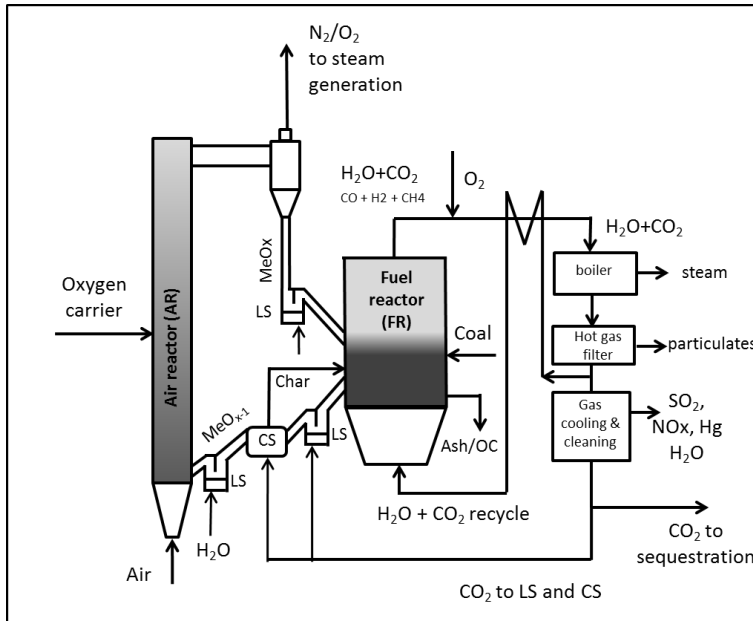


Figure 2. Chemical-looping combustion of coal

A carbon stripper (CS) is therefore required to separate the char from the OC and recirculate it back to the FR. Volatiles in the coal released into the freeboard of the FR often do not have sufficient contact time with the OC and therefore leave the FR unconverted. Oxygen is introduced into the hot gas stream leaving the FR resulting in complete combustion of the volatiles in a post combustion chamber to form CO_2 and H_2O . This step is often referred to as oxygen polishing. After oxygen polishing, fly-ash is removed from the gas using a hot gas filter (ceramic filter or cyclone). To increase the efficiency of the system a portion of the flue gas exiting the hot gas filter is recycled to the FR via a recuperating heat exchanger. This step avoids steam generation and pre-heating of the reactants (CO_2 and H_2O) for the fuel reactor.

During CLC of solids fuels such as high-ash coals, periodic draining of the FR bed will be required to avoid accumulation of ash in the system. Systems have been proposed to separate the OC from the ash and recycle it back to the bed. Due to inefficiencies in these systems some OC loss with the ash will inevitably occur. The ash and sulphur in the coal can in some cases [4] deactivate the OC and it is necessary to add fresh oxygen carrier to the system. It is therefore required to use a low-cost OC, of which abundant reserves are available such as ilmenite, haematite and manganese oxide which are naturally occurring mineral oxides. Synthetically manufactured OC would be more suitable for gas combustion. Ilmenite, which is an abundant mineral, has received the most attention for the CLC of coal due to its ability to maintain its reactivity and structural integrity during many oxidation-reduction cycles. Ilmenite was therefore selected as the OC for this study. Bench and pilot-scale reactors ranging from 25 - 1000 kW_{th} have been constructed and operated using coal as fuel and ilmenite as the oxygen carrier. [5 - 8, 3].

FUEL REACTOR MODELLING

Efforts at modelling the fuel reactor of chemical-looping coal combustion reactors started in earnest after 2007 when the potential of this process was being realized. Models that have been developed can be divided mainly into semi-empirical models which are based on the two-phase theory of fluidisation [9-13], and computational fluid dynamic (CFD) models based on Eulerian and Discrete element method (DEM) approaches [14-18]. CFD models can give a more accurate hydrodynamic simulation of the bed regarding solid volume fraction distribution, velocity distributions and gas-

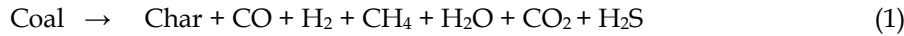
solids flow patterns compared to the two- phase theory of fluidisation. The modelling approach used in this study is a semi-empirical model based on the two-phase theory of fluidisation. The advantages of semi-empirical models are that computational time and cost are lower than CFD models. The computational times of semi-empirical models are in the order of hrs whereas for the CFD models computational times are in the order of weeks. The semi-empirical models are therefore currently more suitable for carrying out sensitivity studies of the process.

Model development

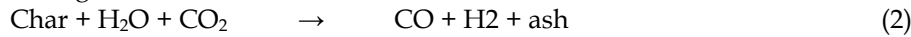
A semi-empirical model [19] previously developed at the CSIR for fluidised bed coal gasification was adapted so that it could be used for the simulation of a CLC fuel reactor. The changes made to the coal gasification model to allow simulation of FR are associated mainly with the reaction kinetics, heat and mass balances and the solution procedures

The reactions in the gasification model which apply to the fuel reactor model are:

Coal devolatilization:



Char gasification:

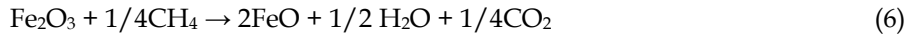


Water-gas shift reaction:



Reactions added to the gasification model to allow simulation of the fuel reactor are:

Redox reactions:



The following assumptions have been added to the gasification model assumptions to facilitate modelling of the fuel reactor.

- Oxygen from the oxygen carrier does not react directly with the coal by an oxygen uncoupling (CLOU) reaction mechanism.
- The conversion of coal takes places by in-situ gasification of char with CO_2 and H_2O (reaction (2)).
- The CO and H_2 produced by gasification of the coal react with the oxygen carrier to produce CO_2 , H_2O and the reduced oxygen carrier (reactions (4) - (6)).
- Ilmenite has an oxygen carrying capacity of 3.3 % can be represented by 33 wt.% Fe_2O_3 and 67 wt.% FeTiO_3 [15].
- The high circulation rate of solids (OC) between the FR and AR does not affect the hydrodynamics of the FR as described by the two phase theory of fluidisation. [19]
- The reaction of steam with the reduced oxygen carrier has not been included in the FR model.

Redox reaction kinetics

Kinetic rate equations are required to calculate the rate of the redox reactions in the FR model. The first order rate equations that were selected to calculate the rate of redox reactions (4) to (6) is given by equations (7) - (9).

$$\frac{dX_{OC}}{dt} = k_{0H_2} \exp\left(\frac{-E_{H_2}}{RT}\right) p_{H_2} (1 - X_{OC})^{\beta_{H_2}} \quad (7)$$

$$\frac{dX_{OC}}{dt} = k_{0CO} \exp\left(\frac{-E_{CO}}{RT}\right) p_{CO} (1 - X_{OC})^{\beta_{CO}} \quad (8)$$

$$\frac{dX_{OC}}{dt} = k_{0CH_4} \exp\left(\frac{-E_{CH_4}}{RT}\right) p_{CH_4} (1 - X_{OC})^{\beta_{CH_4}} \quad (9)$$

Thermogravimetric analyser (TGA) kinetic data [20] for Norwegian ilmenite was used to obtain the parameter values (k_0 , E and β) for the redox rate equations. Before TGA analysis the ilmenite was activated by subjecting it to four reduction /oxidation cycles using CH_4 as the reducing gas and air as the oxidizing gas. Figure 3 shows that the rate equations provide an adequate prediction of the TGA oxygen carrier reduction data. Parameter values for the redox equations derived from the experimental TGA data are given in Table 1.

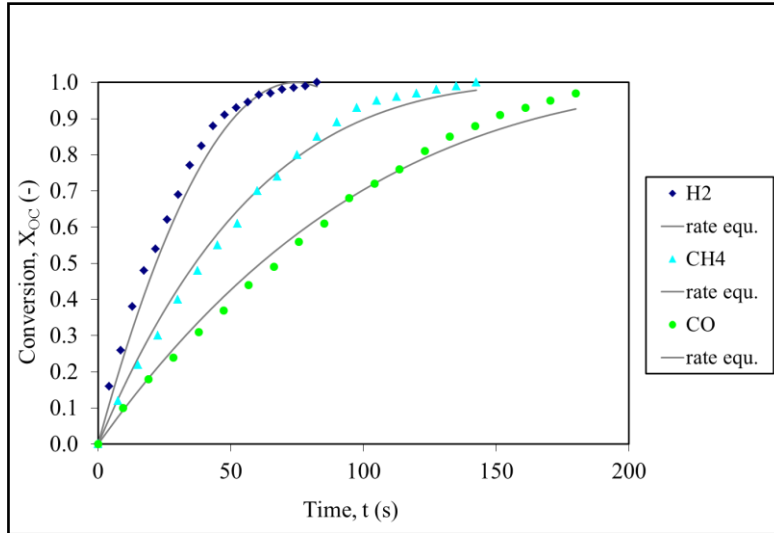


Figure 3. Oxygen carrier conversion as a function of time with reacting gasses H_2 , CH_4 and CO at $900^\circ C$ and atmospheric pressure. Reacting gas mixtures, 15% H_2 +20 % H_2O , 15% CO +20 % CO_2 , 15% CH_4 +20 % H_2O , Balance N_2 .

Table 1. Parameters for the redox reactions of activated Norwegian ilmenite

Reacting gas	$E(KJ/mol)$	$Ln(k_0) (atm^{-1}s^{-1})$	β
H_2	184	17	0.47
CO	252	23	0.72
CH_4	223	20.7	0.75

Parameters for the rate equations to calculate the rate of reactions (1) – (3) are given in reference [21].

Model formulation and solution procedure

Formulation of the model equations is based on mass and energy balances over an incremental horizontal section of the bed with a thickness of Δz as shown in Figure 4. The figure shows that the outlet flows and temperature from an incremental horizontal section of the bed are the inlet flows to the next incremental section.

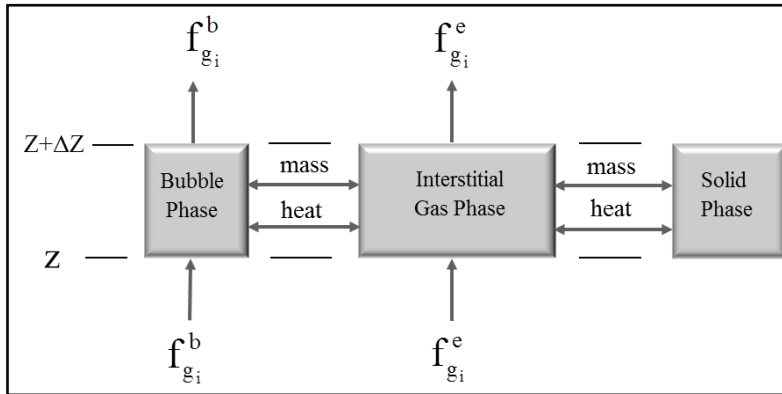


Figure 4. Incremental horizontal section of the fluidised bed

The incremental mass and energy equations produce 16 first-order ordinary differential equations. The independent variable is the height in the fluidised bed (z) and the dependent variables are:

- Molar flowrates of O_2 , N_2 , CO_2 , H_2O , H_2 , CO , and CH_4 in the bubble and emulsion phases ($f_{g_i}^b$ and $f_{g_i}^e$ for $i = 1, 2, \dots, 7$).

Temperature of the bubble and emulsion phases (T^b and T^e)

The system of differential equations is solved using the MATLAB ode45 solver which gives the values of the dependant variables as a function of bed height (z). To calculate the fixed carbon conversion (X_C), the oxygen carrier conversion (X_{OC}) and the solids temperature (T_s), three iteration loops are used as shown in Figure 5. For the FR model, the third iteration loop for the oxygen carrier conversion (X_{OC}) is added to the fixed carbon conversion (X_C) and

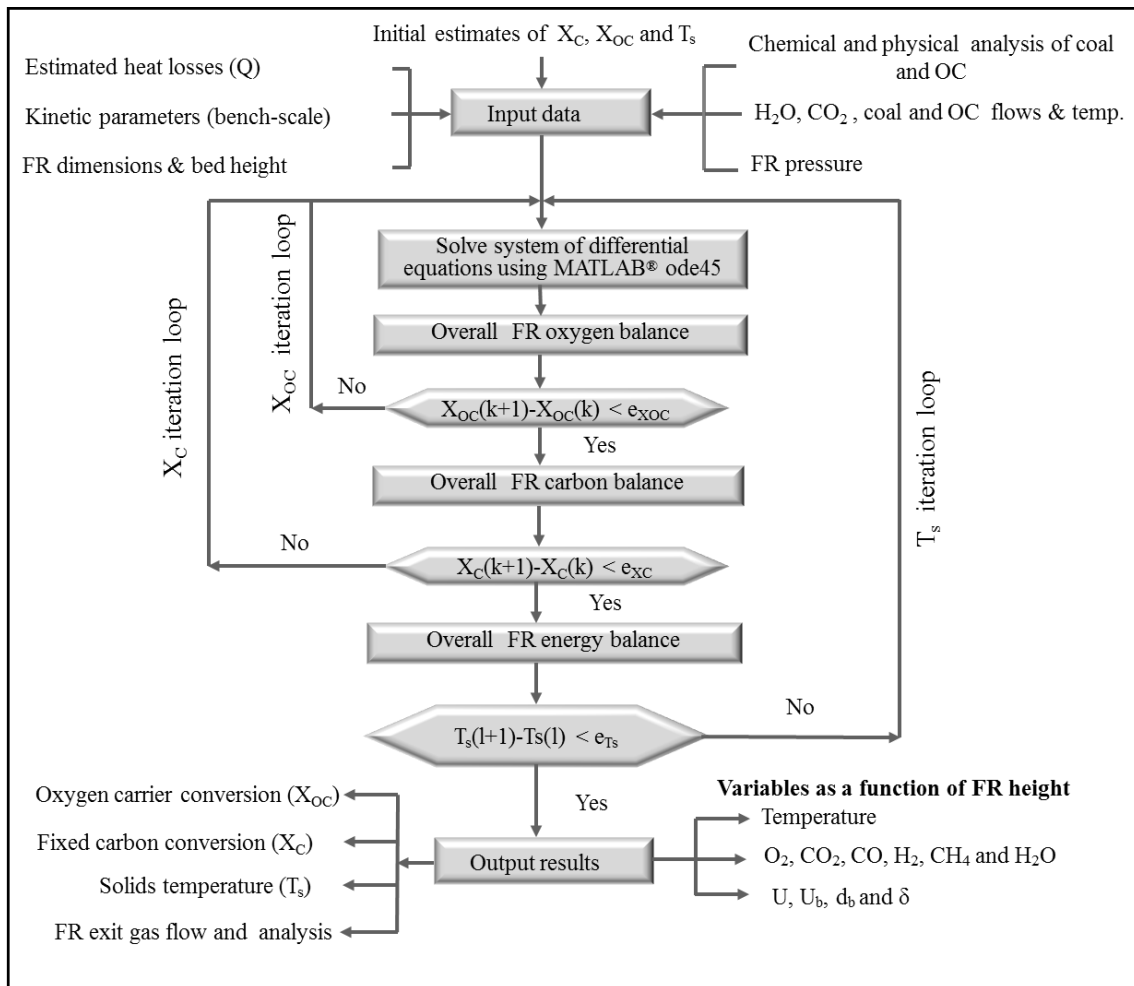


Figure 5. Flowchart of the FR model computational procedure

solids temperature (T_s) of the gasification model. Convergence of all three of the iteration loops was achieved with computational times varying between one and two hrs.

The coal gasification model on which the chemical-looping combustion model is based, was validated using a pilot-scale fluidised bed coal gasifier at the CSIR. The CLC model is in the process of validation using a bench-scale fluidised bed reactor.

SIMULATION OF THE FUEL REACTOR

The CLC model was applied to investigate the chemical-looping combustion of two high-ash South African coals using ilmenite as the oxygen carrier. The design of the fuel reactor on which the investigation is based is given in Table 2.

Table 2. Fuel reactor specification

Specification	Value
Reactor configuration	Bubbling fluidised bed
Bed section dimension	1m x 1m
Bed section height	2 m
Freeboard section dimension	2m x 2m
Free board section height	2 m
Fuel reactor total height	4 m

The *fixed* operating conditions used for the FR simulations are given in Table 3.

Table 3. Fuel reactor operating conditions for simulation

Operating conditions (Fixed values)	Value
Coal feedrate (kg/h)	300 NV/225 GG
Dynamic bed height (m)	1.75
Temperature of OC recycled to FR (°C)	1000
Coal particle size (mm)	0.7
Ilmenite particle size (mm)	0.25
Bed section heat losses (MJ/h)	45

A fixed coal feedrate of 300 kg/h was selected for NV since this would be approximately the coal feedrate to a 1 m² bubbling fluidised bed combustion boiler operating at 860 °C, producing 1360 kg/h of steam at 70 bar pressure. The fluidising velocity would be 2.5 m/s and the excess air 50 %. To produce the same thermal output the feedrate of GG coal to the FB combustor would be 225 kg/h. The maximum safe operating temperature of the AR to avoid sintering of the ilmenite was estimated to be < 1020 °C. The temperature of the OC flowing from the AR to the FR was therefore fixed at 1000 °C.

The *variable* operating conditions used for the FR sensitivity analysis is given in Table 4.

Table 4. Fuel reactor operating conditions for sensitivity analysis

Operating conditions (Variable values)	Value
Temperature (C)	875-950
Solids circulation rate (t/h)	15 -35
Steam concentration of reactants (%)	20 - 80
Temperature of reactants (°C)	200 - 600
Superficial gas velocity (m/s)	1.0 - 1.71
Pressure (kPa)	90 - 1000
Coal reactivity(-)	NV& GG
Ilmenite relative reactivity (-)	0 - 10

The analysis of Grooetegeluk (GG) and New Vaal (NV) coal used for the FR simulations is given in Table 5.

Table 5. Analysis of New Vaal and Grootegeluk coals (air-dried)

	New Vaal	Grootegeluk
Proximate analysis		
Calorific value (MJ/kg)	14.84	21.4
Ash content (wt.%)	40.70	31.7
Moisture (wt.%)	5.70	1.90
Volatile matter (wt.%)	20.50	28.3
Fixed carbon (wt.%)	33.10	38.10
Total sulphur (wt.%)	0.84	1.17
Ultimate analysis:		
Carbon (wt.%)	39.25	52.93
Hydrogen (wt.%)	3.45	4.11
Nitrogen (wt.%)	0.90	1.19
Sulphur (wt.%)	0.84	1.17
Oxygen (wt.%)	9.16	7.00
Reflectance analysis:		
Vitrinite random reflectance (%)	0.55	0.71

The performance of the fuel reactor was evaluated in terms of the following performance variables:

Fixed carbon conversion (X_T)

The total fixed carbon conversion is the percentage of fixed carbon in the coal that is converted to CO₂ exiting the oxygen combustion chamber after the fuel reactor.

CO₂ capture efficiency (η_{cc})

The CO₂ capture efficiency is the percentage of total carbon in coal that is converted to CO₂ exiting the oxygen combustion chamber after the fuel reactor.

Oxygen demand (Ω_T)

The total oxygen demand of the CLC process is the fraction of oxygen required to combust the CO, H₂ and CH₄ in the gasses exiting the FR with respect to that required for stoichiometric combustion of the coal, expressed as a percentage.

Simulations using New Vaal coal

New Vaal coal, which currently supplies the 3.6 GW Lethabo pulverised fuel fired power station, is situated on the banks of the Vaal river in the Free state Province of South Africa. Gasification tests carried on New Vaal coal [21] shows that it has a significantly higher gasification reactivity than GG coal (bituminous) which has a reactivity that is representative of the feed coal to the majority of power stations in South Africa. The reactivity of New Vaal coal is similar to the reactivity of some lignite coals.

Oxygen carrier circulation rate

Figure 6 shows that increasing the circulation rate of OC between the FR and AR from 15 t/h to 35 t/h increases the FR temperature from 875 °C to 940 °C. The increase in FR temperature results in an increase fixed carbon conversion (X_T) from 74 % to 91 %. The CO₂ capture efficiency (η_{cc}) increases from 78 % to 93 %. Increasing the OC circulation rate has the advantage of increasing the FR temperature; the disadvantage is that the char residence time in the FR decreases since the char is continuously removed from the FR with the circulating OC (Figure 7). This explains why when increasing the OC circulation rate from 25 t/h to 35 t/h, only increases X_T from 89 to 91 %. CLC

reactors that are used for gas (CH_4 and syngas) combustion do not suffer from this disadvantage. Figure 6 shows that the rate at which the FR temperature increases, is lower at higher FR temperatures. At higher FR temperatures the amount of heat that is transferred to the FR by the OC is lower since the temperature difference (ΔT) between the AR and FR is lower.

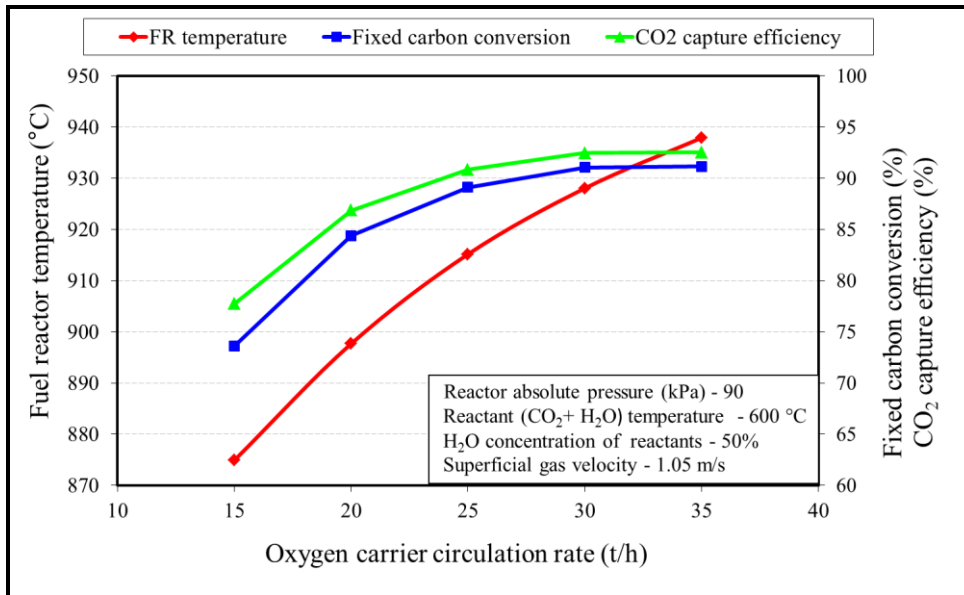


Figure 6. FR temperature, X_T and η_{cc} as a function of OC circulation rate (NV coal)

Investigations have been carried out [3, 22, 23] that included a carbon stripper (CS) between the FR and the AR for separation and recycle of char back to the FR. Challenges experienced with the CS are low separation efficiencies and cooling of the circulating OC stream. For this study, a CS was not considered since it would have resulted in significantly longer computational times.

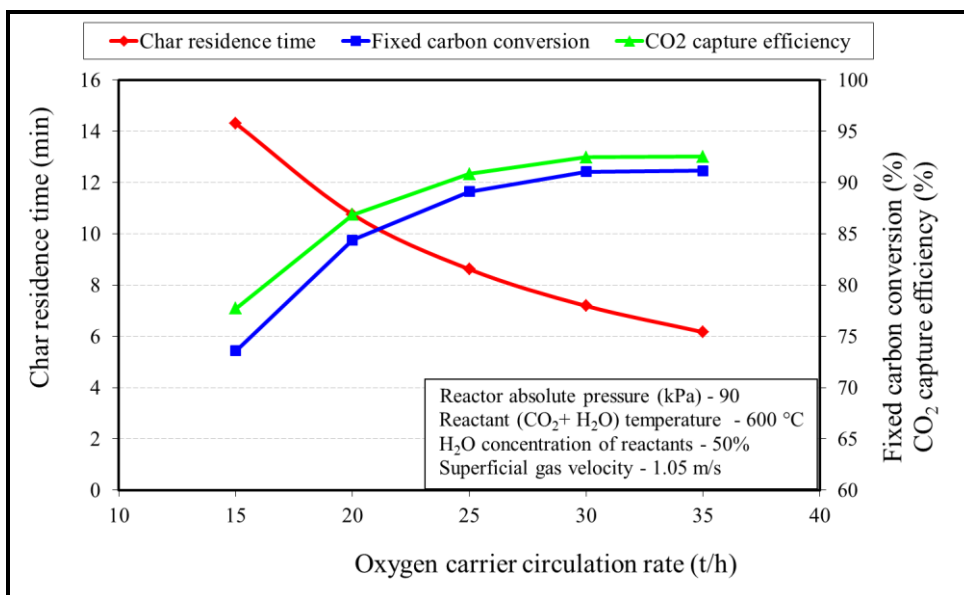


Figure 7. Char residence time, X_T and η_{cc} as a function of OC circulation rate (NV coal)

Increasing the OC circulation rate from 15 t/h to 35 t/h resulted in a decrease in the oxygen demand (Ω_T) of the process from 4.1 % to 1.7 %. The higher fixed carbon conversion and FR temperature at

higher OC circulation rates results in lower concentrations of CO, H₂ and CH₄ in the freeboard of the FR and therefore a lower oxygen demand of the post combustion chamber.

Steam concentration of fluidizing gas

Table 6 shows that due to the higher reactivity of H₂O with char than CO₂ with char, the fixed carbon conversion increases as the concentration of H₂O in the fluidising gas to the FR increases. For H₂O concentrations in the flue gas above 50 %, the rate of increases in X_T above 90 % is low. The rate of the steam char gasification reaction slows down as 100 % conversion is approached as described by the structural factor in the Johnson H₂O-char rate equation [21].

Table 6. Effect of fluidising gas steam concentration (NV coal)

	Steam concentration (%)			
	20	40	60	80
Performance variables				
Temperature (C)	918	915	913	912
X _T - Fixed carbon conversion (%)	82.0	87.2	90.1	91.5
η _{cc} - CO ₂ capture efficiency (%)	84.8	89.2	91.6	92.9
Ω _T - Oxygen demand (%)	2.30	2.31	2.30	2.28
Oxygen carrier conversion (%)	39.2	40.3	40.9	41.3
Constant values				
OC circulation rate (t/h)	25.0	25.0	25.0	25.0
Char residence time (min)	8.62	8.62	8.62	8.62
Superficial gas velocity (m/s)	1.05	1.05	1.05	1.05
FR absolute pressure (kPa)	90.0	90.0	90.0	90.0
Fluidising gas temperature (°C)	600	600	600	600

In steam-char gasification systems, it is therefore difficult to achieve conversions of higher than 95 %. In coal combustion systems fixed carbon conversions of higher than 95 % are often achieved since the combustion rate is controlled by diffusion of oxygen to the particle and not by intrinsic combustion kinetics

Temperature of fluidising gas

Table 7 shows that increasing the fluidising gas temperature from 200 °C to 800 °C increases the temperature from 901 °C to 921 °C and the fixed carbon conversion from 82.8 % to 90.6 %. The fluidising gas temperature has a lower effect on the performance of the FR than the OC circulation rate since the majority of the sensible heat input (75 %) to the fuel reactor is supplied by the circulating oxygen carrier and only 25 % (at 800 °C pre-heat) by the sensible heat in the fluidising gas stream.

Table 7. Effect of fluidising gas temperature (NV coal)

	Temperature (°C)			
	200	400	600	800
Performance variables				
Temperature (C)	901	907	914	921
X _T - Fixed carbon conversion (%)	82.8	86.0	88.7	90.6
η _{cc} - CO ₂ capture efficiency (%)	85.5	88.2	90.5	92.0
Ω _T - Oxygen demand (%)	2.6	2.5	2.3	2.1
Oxygen carrier conversion (%)	39.3	40	40.7	41.1
Constant values				
OC circulation rate (t/h)	25.0	25.0	25.0	25.0

Char residence time (min)	8.62	8.62	8.62	8.62
Superficial gas velocity (m/s)	1.05	1.05	1.05	1.05
FR absolute pressure (kPa)	90.0	90.0	90.0	90.0
Steam concentration of fluidising gas (°C)	50.0	50.0	50.0	50.0

Superficial gas velocity

Table 8 shows that as the superficial gas velocity is increased from 1.05 m/s to 1.71 m/s the fixed carbon conversion decreases from 88.8 % to 80.9 %. An increase in the superficial gas velocity results in an increase in the bubble fraction of the bed. At a fixed dynamic bed height of 1.75 m, this will result in a lower bed hold-up, a lower char residence time and subsequently a lower fixed carbon conversion.

Table 8. Effect of superficial gas velocity (NV coal)

	Superficial gas velocity (m/s)		
	1.05	1.38	1.71
Performance variables			
Temperature (°C)	914	910	907
X _T - Fixed carbon conversion (%)	88.8	85.4	80.9
η _{cc} - CO ₂ capture efficiency (%)	90.5	87.7	83.9
Ω _T - Oxygen demand (%)	2.3	3.0	4.0
Oxygen carrier conversion (%)	40.7	39.7	38.5
Char residence time (min)	8.6	7.7	6.9
Constant values			
OC circulation rate (t/h)	25.0	25.0	25.0
FR absolute pressure (kPa)	90	90	90
Fluidising gas temperature (°C)	600	600	600
Steam concentration of fluidising gas (°C)	50.0	50.0	50.0

Ilmenite relative reactivity

Table 9 shows simulation runs using activated Norwegian ilmenite with a reactivity of 1 and for ilmenite having reactivities of 1/2, 1/4, 1/10 and 0 relative to activated Norwegian ilmenite. The results show that at 1/10 of the reactivity of the base case the fixed carbon conversion decreases by 10 %. A higher OC reactivity enhances the rate of the gasification reactions since the gasification products CO and H₂, which are known to inhibit the gasification reactions, are consumed at a higher rate by the redox reaction. A case was also run using silica sand as bed material (reactivity = 0) to investigate the performance of the FR without the presence of redox reactions. This would represent the case of a dual fluidised bed gasifier. The results show that the fixed carbon conversion decreases to 50.7 %. In this case, the unconverted char is fed to the AR (combustor) to heat the recirculating sand to 1000 °C before it is returned to FR. The high oxygen demand of 64 % is as a result of the high CO (19.74 %), H₂ (13.72 %) and CH₄ (1.21 %) concentration of the gas leaving the FR.

Table 9. Ilmenite reactivity (NV coal)

	Ilmenite relative reactivity				
	0	1/10	1/4	1/2	1
Performance variables					
Temperature (°C)	941	920	917	915	914
X _T - Fixed carbon conversion (%)	50.7	77.2	83.4	86.7	88.8
η _{cc} - CO ₂ capture efficiency (%)	58.5	80.8	86.0	88.8	90.5
Ω _T - Oxygen demand (%)	64.0	11.9	6.3	3.7	2.3
Oxygen carrier conversion (%)	0	35.3	38.3	39.8	40.7
Constant values					
OC circulation rate (t/h)	25.0	25.0	25.0	25.0	25.0
Char residence time (min)	8.62	8.62	8.62	8.62	8.62
Superficial gas velocity (m/s)	1.05	1.05	1.05	1.05	1.05
FR absolute pressure (kPa)	90.0	90.0	90.0	90.0	90.0
Fluidising gas temperature (°C)	600	600	600	600	600
Steam concentration of fluidising gas (°C)	50.0	50.0	50.0	50	50

Simulation using optimal operating conditions

The above sensitivity analysis indicated that the approximate optimal operating conditions for the selected FR configuration (Table 2) and fixed operating conditions (Table 3) are:

- Oxygen carrier circulation rate (kg/h) - 25 000
- Temperature of fluidising gas (°C) - 600
- Steam concentration of fluidizing gas (%) - 50
- Superficial gas velocity (m/s) - 1.1

A simulation was carried out using NV coal, activated Norwegian ilmenite and the optimum FR operating conditions. The output of the simulation (Figure 8) is shown in the form of a flow diagram of a 1.3 MW_{th} CLC power station. The flow diagram shows that the AR and the FR have separate heat recovery trains that are used for steam generation and gas pre-heating. The majority of the heat (± 70 %) is released from the AR which produces 852 kg/h steam in a boiler. The remainder of the heat from the AR is used to pre-heat the combustion air for the AR to 300 °C. The heat that is released from the FR is used to pre-heat the fluidising gas (CO₂ & H₂O) to the FR to 600 °C and to generate 373 kg/h steam in a boiler. The steam from the AR and FR boilers are combined and used to generate 430 kW of AC power assuming a steam turbine and generator efficiency of 45 %. The overall coal to electrical efficiency on a HHV basis is 32.6 %.

The flue gas from the AR contains mainly N₂ and O₂. A low amount of thermal NO_x would be produced in the AR due to the low combustion temperature (1000 °C) compared to pulverised coal combustion. Assuming no coal char flows from the FR to the AR no fuel NO_x would be produced in the AR. After filtering a portion of the flue gas from the FR is used as fluidising gas for the FR. The remainder of the FR off gas is purged from the system and after water removal, contain > 99 % CO₂. Due to the high CO₂ concentration of the purge gas, it would require little further treatment to produce a sequestrable CO₂ stream.

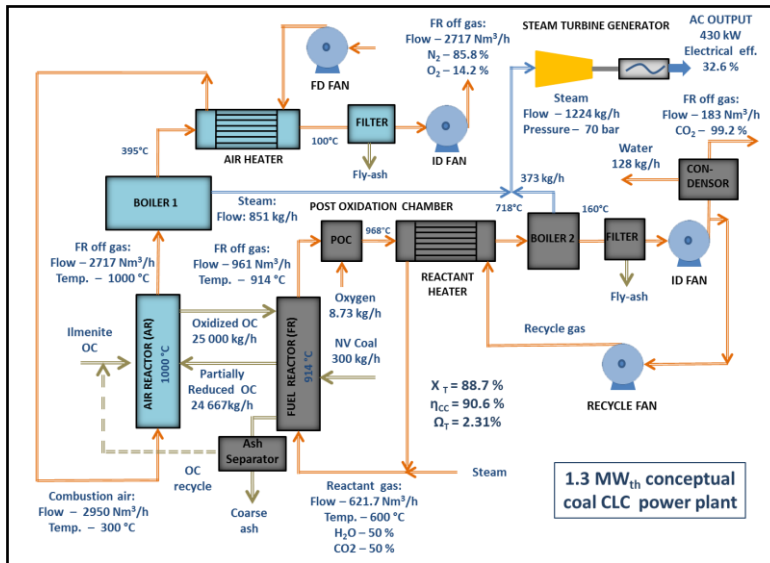


Figure 8. Coal Chemical-looping combustion power plant (1.3 MW_{th})

Simulations using Grootegeluk coal

Chemical-looping combustion simulations were carried out using GG coal which has char reactivity that is similar to most power station coals in South Africa.

Oxygen carrier circulation rate

Figure 9 shows that an increase in the OC circulation rate increases the temperature and fixed carbon conversion as observed with NV coal. However, due to the lower reactivity of GG coal, the fixed carbon conversion is low at ± 55 % which is 36 % lower than the ± 91 % fixed carbon conversion achieved with NV coal. The relative reactivity factor (f_L) for GG in the Johnson steam-char rate equation is 1.2 compared to 8.95 for NV coal.

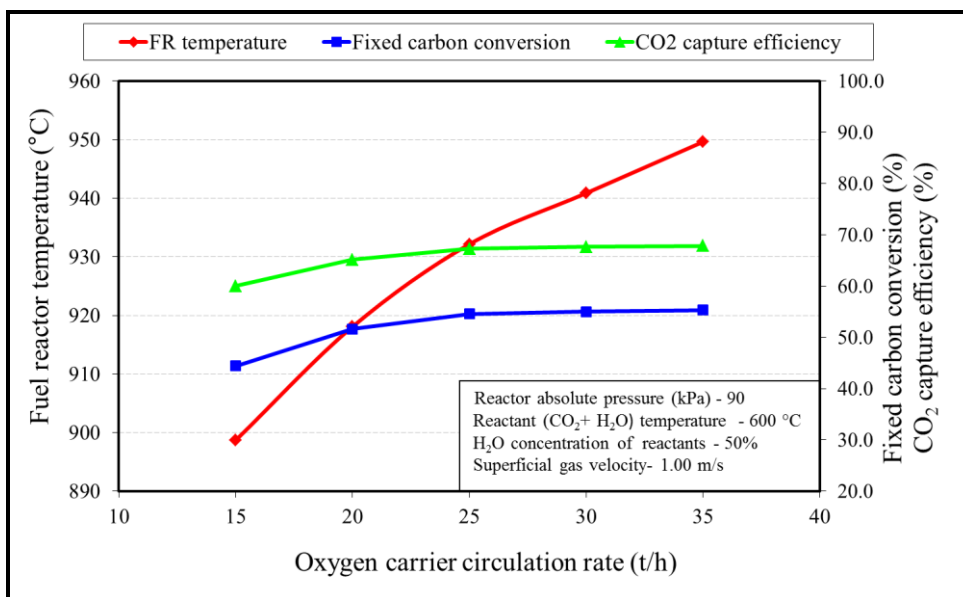


Figure 9. FR temperature, X_T and η_{CC} as a function of OC circulation rate (GG coal)

Figure 10 shows that the decrease in char residence time with an increase of OC circulation rate has a greater negative effect on the fixed carbon conversion than in the case of NV coal. This is again due to the lower reactivity on GG coal compared to NV coal.

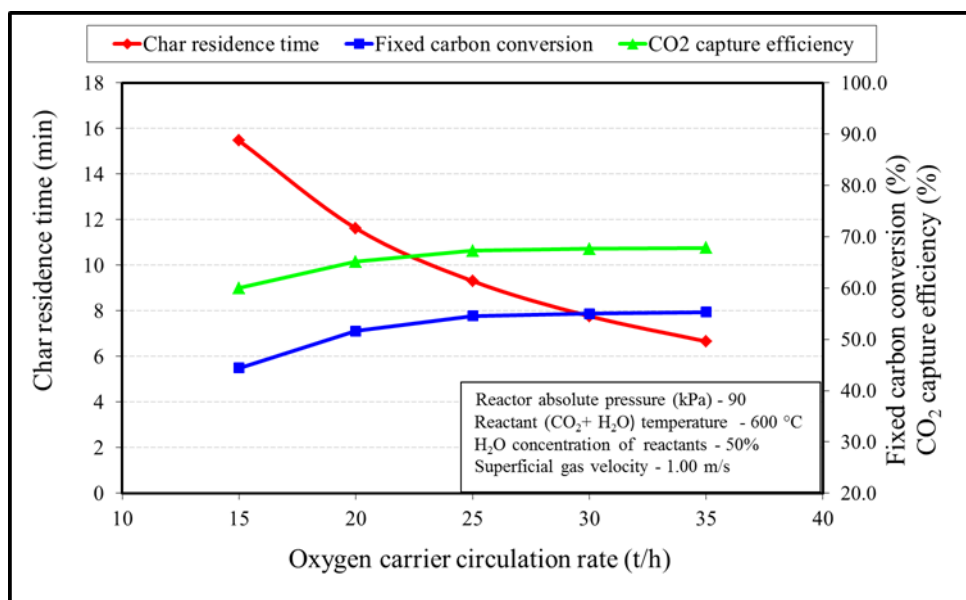


Figure 10. Char residence time, X_T and η_{cc} as a function of OC circulation rate (GG coal)

Steam concentration, temperature and velocity of the fluidising gas

The above operating variables have a similar trend on performance variables as shown for NV coal in Tables 6 - 9 and have therefore not been presented here. The average difference in X_T between NV and GG is in all cases $\pm 35\%$.

Fuel reactor pressure

Simulations were carried out with FR pressures of 500 kPa and 1000 kPa to investigate the effect on FR performance. Table 10 shows that at 1000 kPa the fixed carbon conversion increased to 78.5%. This can be attributed to the higher rate of the steam-char and CO₂-char gasification reactions and the longer residence times at higher pressure. At higher pressures, the char residence times increase due to the lower bubble fraction of the bed and resulting higher mass of char in the bed (hold-up). To operate the FR and the AR of a chemical-looping combustor under pressure, practical considerations, such as being able to control the OC circulation rate and the temperature of the FR has to be taken into consideration.

Table 10. Char residence time, X_T and η_{cc} as a function of OC circulation rate

Performance variables	FR pressure (kPa)		
	90	500	1000
Temperature (°C)	932	899	908
X_T - Fixed carbon conversion (%)	54.6	69.5	78.5
η_{cc} - CO ₂ capture efficiency (%)	67.3	78.0	84.6
Ω_T - Oxygen demand (%)	1.6	1.2	1.0
Oxygen carrier conversion (%)	35.5	46.4	48.7
Constant values			

OC circulation rate (t/h)	25.0	25.0	25.0
Steam concentration of fluidising gas (°C)	50.0	50.0	50.0
Fluidising gas temperature (°C)	600	600	600
Variable values			
Char residence time (min)	9.11	12.92	13.39
Superficial gas velocity (m/s)	1.02	0.33	0.28

SUMMARY AND CONCLUSIONS

A mathematical model based on the two-phase theory of fluidisation for bubbling fluidised beds was developed to simulate the chemical-looping combustion of coal. The model was applied to simulate the chemical-looping combustion of two high-ash South African coals using ilmenite as the oxygen carrier. The simulation results show that fixed carbon conversions of up to 90 % can be achieved using NV without recycling of char to the fuel reactor. The effect of operating variables on the performance of the fuel reactor was investigated. These operating variables were oxygen carrier circulation rate, steam concentration, the temperature of the fluidising gas and superficial gas velocity. It was found that initially, an increase in the oxygen carrier circulation rate increased fixed carbon conversion. Above an optimum oxygen carrier circulation rate no further increase in the fixed carbon conversion was predicted by the model. This can be attributed to the lower char residence times at higher oxygen carrier circulation rates and the decrease in the rate of the gasification reactions at higher fixed carbon conversions. An increase in the temperature and steam concentration of the fluidising gas had a beneficial effect on the performance of the fuel reactor up to a point beyond which further increases have no beneficial effect. The model shows that higher oxygen carrier reactivity results in higher fixed carbon conversions since the reaction products of char gasification (CO, H₂ and CH₄), which inhibit the rate of the gasification reactions, are consumed at a higher rate by the redox reactions.

Simulation using GG coal and activated Norwegian ilmenite as the oxygen carrier shows that fixed carbon conversions are limited to ± 55 % due to the lower char reactivity of GG coal. The model predicts that the fixed carbon conversion can be increased to ± 80 % if the fuel reactor is operated at a pressure of 1000 kPa (10 bar). This is due to the higher rate of the gasification and redox reaction at a higher pressure and also due to the higher bed density. In future simulation will be carried out to investigate the effect of char stripping (CS) and char recycle on the performance of the fuel reactor. Further changes to the model will be made to simulate a FR operating in the fast fluidisation regime.

NOTATION

E_{H_2}	Arrhenius activation energy of the OC-H ₂ reaction	$\text{kJ}\cdot\text{mol}^{-1}$
E_{CO}	Arrhenius activation energy of the OC-CO reaction	$\text{kJ}\cdot\text{mol}^{-1}$
E_{CH_4}	Arrhenius activation energy of the OC-CH ₄ reaction	$\text{kJ}\cdot\text{mol}^{-1}$
e_{Ts}	convergence criteria for solids temperature	°C
e_{xc}	convergence criteria for fixed carbon conversion	-
e_{xoc}	convergence criteria for oxygen carrier	-
f_g^b	flowrate of bubble phase gas	$\text{mol}\cdot\text{s}^{-1}$
f_g^e	flowrate of emulsion phase gas	$\text{mol}\cdot\text{s}^{-1}$
f_{gi}^b	flowrate of gas component i in the bubble phase	$\text{mol}\cdot\text{s}^{-1}$
f_{gi}^e	flowrate of gas component i in the emulsion phase	$\text{mol}\cdot\text{s}^{-1}$
f_L	relative reactivity factor in the Johnson rate equation	-
k_{0H_2}	pre-exponential factor of the OC-H ₂ reaction	$\text{atm}^{-1}\cdot\text{s}^{-1}$
k_{0CO}	pre-exponential factor of the OC-CO reaction	$\text{atm}^{-1}\cdot\text{s}^{-1}$
k_{0CH_4}	pre-exponential factor of the OC-CH ₄ reaction	$\text{atm}^{-1}\cdot\text{s}^{-1}$
p_{H_2}	partial pressure of gas H ₂ the gas	atm
p_{CO}	partial pressure of gas CO the gas	atm

p_{CH_4}	partial pressure of gas CH_4 the gas	atm
Q	FR energy losses	$\text{MJ}\cdot\text{h}^{-1}$
T^b	bubble temperature	$^\circ\text{C}$
T^e	emulsion temperature	$^\circ\text{C}$
T_s	solids temperature	$^\circ\text{C}$
ΔT	temperature difference between the FR and AR	$^\circ\text{C}$
U	superficial gas velocity	$\text{m}\cdot\text{s}^{-1}$
U_b	bubble velocity	$\text{m}\cdot\text{s}^{-1}$
X_{OC}	fractional conversion of oxygen carrier	-
X_{T}	percentage conversion of fixed carbon in coal	(%)
ΔZ	height of an incremental bed section	m
Z	height in the fluidised bed	m

Greek letters

β	grain model structural parameter	-	-
δ	bubble fraction of the bed		
η_{cc}	CO_2 capture efficiency		
Ω_{T}	Oxygen demand		

Acronyms/Abbreviations

GG	Grootegeeluk
NV	New Vaal
FR	Fuel Reactor
AR	Air Reactor
CLC	Chemical-Looping Combustion
OC	Oxygen Carrier
TGA	Thermogravimetric Analyser/ Analysis
CS	Carbon Stripper
LS	Loop Seal
CLOU	Chemical-Looping combustion with Oxygen Uncoupling
FD	Forced Draught
ID	Induced Draught

ACKNOWLEDGEMENTS

The authors would like to extend their appreciation to the Council for Scientific and Industrial Research for providing financial support.

REFERENCES

1. Fan, J., Zhui, L., Hong, H., Jiang, Q., Jin, H. (2017). A thermodynamic and environmental performance of in-situ gasification of chemical-looping combustion for power generation using ilmenite with different coals and comparison with other coal driven power technologies for CO_2 capture. *Energy* 119: 1171-1181.
2. Erlach, B., Schmidt, M., Tsatsaronis, G. (2010). Comparison of carbon capture IGCC with pre-combustion decarbonisation and with chemical-looping combustion. *Energy* 36: 3804-3815.
3. Ströhle, J., Orth, M., Epple, B. (2015). Chemical-looping combustion of hard coal in a 1 MW_{TH} pilot plant using ilmenite as oxygen carrier. *Applied Energy* 157: 288-294.
4. Keller, M., Arjmand, M., Leion, H., Mattisson, T. (2014). Interaction of Mineral Matter of Coal with Oxygen Carriers in Chemical-Looping Combustion (CLC). *Chemical Engineering Research and Design* 92: 1753 - 1770.

5. Thon, A., Kramp, M., Hartege, E., Heinrich, S., Werther, J. (2014). Operational experience with a system of coupled fluidised beds for chemical-looping combustion of solid fuels using ilmenite as oxygen carrier. *Applied Energy* 118: 309-317.
6. Abad, A., Pérez-Vega, R., De Diego, L.F., García-Labiano, F., Gayà, P., Adànez, J. (2015). Design and operation of a 50 kWth Chemical-looping Combustion (CLC) unit for solid fuels. *Applied Energy* 157: 295-303.
7. Lynfeldt, A., Linderholm, C. (2014). Chemical-Looping Combustion of Solid Fuels – Technology Overview and Recent Operational Results in 100 kW Unit. *Energy Procedia* 63: 98–112.
8. Kolbitsch, P., Bolhár-Nordenkampf, J., Pröll, E., Hofbauer, H., (2010). Operating experience with chemical-looping combustion in a 120 kW dual circulating fluidized bed (DCFB) unit. *International Journal of Greenhouse Gas Control* 4: 180-185.
9. Abad, A., Adànez, J., Gayà, P., De Diego, L.F., García-Labiano, F. (2013). Fuel reactor modelling in Chemical-Looping Combustion of coal: 1. Model formulation. *Chemical Engineering Science* 87: 277-293.
10. Abad, A., Adànez, J., Gayà, P., De Diego, L.F., García-Labiano, F. (2013). Fuel reactor modelling in Chemical-Looping Combustion of coal: 2. Simulation and optimization. *Chemical Engineering Science* 87: 173-182.
11. Abad, A., Adànez, J., Cuadrat, A., García-Labiano, F., Gayà, P., De Diego, L.F., Lyngfeldt, A. (2013). Fuel reactor model validation: Assessment of key parameters affecting the chemical - looping combustion of coal. *International Journal of Greenhouse gas control* 19: 541-551.
12. Ohlemüller, P., Alobaid, F., Gunarson, A., Ströhle, J., Epple, B. (2015). Development of a process model for coal chemical-looping combustion and validation against 100 kWth tests. *Applied Energy* 157: 433-448.
13. Peltola, P., Ritvanen, J., Tynjälä, T., Pröll, T., Hyppänen, T. (2013). One-dimensional modelling of chemical-looping combustion in dual fluidized bed reactor system. *International Journal of Greenhouse Gas Control* 16: 72-82.
14. Mahalatkar, K., Kuhlman, J., Huckaby, D., O'Brien, T. (2011). CFD simulation of a chemical-looping fuel reactor utilizing solid fuel. *Chemical Engineering Science* 66: 119-141.
15. Parker, J.M., (2014). CFD model for the Simulation of Chemical-Looping Combustion. *Powder Technology* 265: 47-53.
16. Su, M., Zhao, H., Ma, J. (2015). Computational fluid dynamic simulation for chemical-looping in a dual circulating fluidized bed. *Energy Conversion and Management* 105: 1-14.
17. Alobaid, F., Ohlemüller, P., Ströhle, J., Epple, B. (2015). Extended Euler-Euler model for the simulation of a 1 MW_{TH} chemical-looping pilot plant. *Energy* 93: 2395-2405.
18. Sharma, R., May, J., Alobaid, F., Ohlemüller, P., Ströhle, J., Epple, B. (2017). Extended Euler-Euler model for the simulation of a 1 MW_{TH} chemical-looping pilot plant. Influence of drag models and specular coefficient. *Fuel* 200: 435- 446.
19. Engelbrecht A.D., North B.C., Oboirien B.O., Everson R.C. and Neomagus H.W.P.J. (2014) Fluidized bed gasification of selected high-ash coals. *Proceedings of Industrial Fluidization South Africa*: 135–151. November 2014.
20. Abad, A., Adànez, J., Cuadrat, A., García-Labiano, F., Gayà, P., De Diego, L.F. (2011). Kinetics of redox reactions of ilmenite for chemical-looping combustion. *Chemical Engineering Science* 66: 689-702.
21. Engelbrecht, A.D. (2014). Fluidised bed gasification of high-ash South African coals: An experimental and modelling study. Doctoral thesis. North-West University, South Africa.
22. Kramp, M., Thon, A., Hartege, E., Heinrich, S., Werther, J. (2012). Carbon Stripping – A Critical Process Step in Chemical-looping Combustion of Solid Fuels. *Chemical Engineering Technology* 35: 497– 507.
23. Cheng, M., Li, Y., Li, Z., Cai, N. (2017). An integrated fuel reactor coupled with an annular carbon stripper for coal-fired chemical-looping combustion. *Powder Technology* 320: 519-529.